Landscape Ecol (2021) 36:3591–3606
https://doi.org/10.1007/s10980-021-01330-7

RESEARCH ARTICLE

Drivers of recent forest cover change in southern South America are linked to climate and CO_2

Ayodele Ogunkoya · Jed Kaplan · Cathy Whitlock · William Nanavati · David W. Roberts · Benjamin Poulter

Received: 7 August 2020 / Accepted: 12 August 2021 / Published online: 20 August 2021

Abstract

Abstract and background Widespread changes in forest structure and distribution have been documented in northern Patagonia over the past century. We employed LPJ-GUESS, a dynamic global vegetation model (DGVM) to investigate the role of climate, atmospheric carbon dioxide (CO_2), and fire on simulated forest cover during the twentieth century. Our objective was to assess the drivers responsible for forest change to temperature, precipitation, radiation, fire and atmospheric CO_2

Results Simulations using observed changes in climate and CO_2 from 1930 to 2010, showed an increase in forest cover under changing climate and CO_2, because of higher carbon assimilation and net primary production. The model results were compared with a remote-sensing-derived biomass map and 'greening' indices from the normalized difference vegetation index. Model simulations and satellite data both show increased greening at high and low elevations. In contrast, simulations using pre-industrial climate and CO_2 conditions resulted in a decrease in fire frequency

Supplementary Information The online version contains supplementary material available at https://doi.org/10.1007/s10980-021-01330-7.

A. Ogunkoya (✉) · D. W. Roberts
Department of Ecology, Montana State University, Bozeman, MT 59717, USA
e-mail: ayodelegilbert@gmail.com

J. Kaplan · C. Whitlock
Department of Earth Sciences, University of Hong Kong, Pokfulam, Pokfulam, Hong Kong

C. Whitlock
Montana Institute on Ecosystem, Montana State University, Bozeman, MT 59717, USA

W. Nanavati
Department of Geography, Portland State University, Portland OR 97201 USA

B. Poulter
Biospheric Science Laboratory, NASA Goddard Space Flight Center, Greenbelt, MD 20771, USA

and lower simulated biomass than is reflected by present-day vegetation.

Conclusion Our simulations shows that climate is the primary driver and CO_2 fertilization is the secondary driver of forest expansion in northern Patagonia. We suggest that rising CO_2 mitigates climate-induced drought stress due to increases in water-use efficiency.

Keywords Patagonian forest · Fire suppression · Climate · Dynamic global vegetation models (DGVMs) · Biomass · Atmospheric CO_2

Introduction

Climate, fire, and atmospheric CO_2 constrain and shape the vegetation composition and structure at the landscape scale (Bradshaw and Sykes 2014). These interactions are complex because fuel load, fuel types, and moisture (all elements of a fire regime) are controlled by climate while rising atmospheric CO_2 leads to more efficient photosynthesis and allows less dought-tolerant vegetation (trees) to survive in areas where it may be too dry (Calvo and Prentice 2015). In turn, fire releases carbon from vegetative biomass into the atmosphere creating a complex feedback mechanism between vegetation, fire regime, and climate (van der Werf et al. 2010). Ecosystems thus respond to changes in climate, CO_2, and fire, either by increasing or decreasing biomass production. A process-based ecosystem model can assist in examining these interactions because different drivers of forest productivity (e.g., CO_2, fire, and climate) can be changed one variable at a time (Calvo and Prentice 2015).

The northern Patagonian region of southern South America (Fig. 1) represents an interesting geography to explore the interaction of climate, CO_2, and fire because of the strong climate gradients and vegetation patterns. The north-to-south orientation of the Andes creates west-to-east moisture gradient, which in turn affects forest distribution. The mean elevation of the Patagonian Andes decreases from approximately 3000 m at 38 °S to less than 1000 m at 56 °S. Mean annual temperature, growing season length, species richness, and total above-and below-ground biomass also decrease from north to south. Across the longitudinal

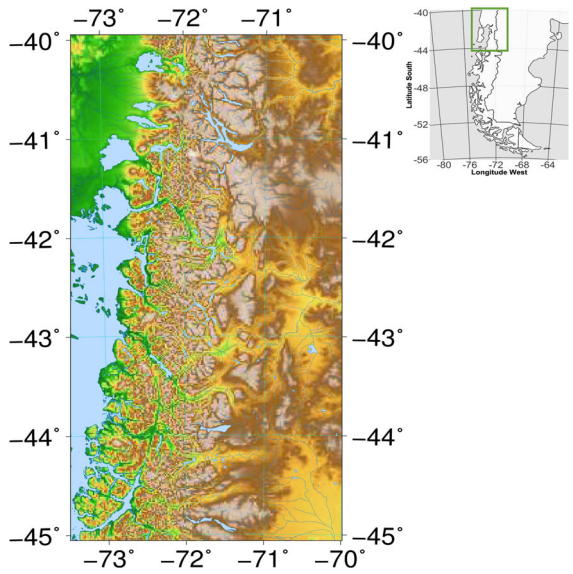

Fig. 1 Map showing the topography of the study area. The Andes influence the west-to east precipitation and vegetation gradient in the region. The west is wetter than the east as a result of orographic precipitation

trans-Andean gradient, annual precipitation decreases from west to east (Veblen et al. 1996).

Tree invasion of the steppe during the 20th century has been described in northern Patagonia based on information from dendroecology, remotely sensed data, repeat photography, and landscape models (Paritsis et al. 2018). Increased *Austrocedrus chilensis* woodland along the Patagonia steppe (40–41 °S) between 1913 and 1985 is hypothesized to be the result of changes in fire and grazing (Veblen and Lorenz 1988). Changes in patch composition and landscape structure (41 °S) from wet forest to the semi-arid woodlands from 1940 and 1970 have been attributed to a reduction in fire frequency (Veblen et al. 1999). Gowda et al. (2011) used historical land-cover maps from 1914 in combination with 30 years of LANDSAT data to quantify the change in forest cover along the northern Patagonia forest-steppe transition and attributed the change to human-related activities (i.e., fire, intensive grazing) and structural features of the landscape (i.e., topography, aspect and slope).

In this paper, we used the Lund-Potsdam-Jena General Ecosystem Simulator (LPJ-GUESS) DGVM, a dynamic process-based model that simulates stands-level eco-physiological processes (i.e., photosynthesis

and respiration) and ecological dynamics (i.e., competition, disturbance). The use of a DGVM allows the exploration of different climate-fire scenarios that might influence vegetation cover and biomass and the role of fire in altering these effects. We address the following questions:

1. How well does LPJ-GUESS simulate present Patagonian vegetation gradients in terms of forest cover?
2. Can the model reproduce observed trends in forest cover over the twentieth century?
3. What is the role of climate, atmospheric CO_2, and fire in forest expansion in the last 115 years?

Study area

The dramatic environmental gradient in northern Patagonia (40–45 °S) is shaped by the rainshadow produced by the interception of the Southern westerly wind belt (SWW) by the Patagonian Andes. The seasonal position and strength of the SWW are determined by the intensity and location of the southern Pacific subtropical atmospheric low-pressure systems (Garreaud et al. 2009). The Andes act as an effective barrier in blocking the movement of the SWW, causing orographic precipitation west of the Andes at high elevations, and dry conditions on the eastern flank of the Andes and into the steppe (Fig. 2) (Paruelo et al. 1998). Along the northern Patagonian Andes, annual precipitation ranges from ~3000 mm/yr^{-1} at the Andean crest to ~500 mm/yr^{-1} in the steppe (Garreaud et al. 2013). In the temperate rainforest west of the Andes, the average annual temperature is 11.1 °C, average austral winter temperature is 7.6 °C (June, July, and August of 1901–2016), and the average austral summer temperature is 15.0 °C (December, January, and February of 1901–2016). However, at high elevation (~1500 m), the average annual temperature is 2.6 °C, average austral winter temperature is − 2.4 °C, average austral summer temperature is 7.9 °C. East of the Andes, at low elevation (~800 m), the average annual temperature is 7.4 °C, and the average austral winter temperature is 1.9 °C; average austral summer temperature is 13.2 °C (Harris et al. 2014). Although ecologically considered a predominately temperate bioclimatic zone (Amingo and Ramirez 1998), two Koppen-Geiger climate classifications described the majority of northern Patagonia: warm temperate fully humid summer on the western flank of the Andes and cold arid steppe to the east (Kottek et al. 2006).

The temperate rainforest is dominated by the shade-intolerant *Nothofagus* species (e.g. *N. alpina*), the coniferous *Fitzroya cupressoides*, and shade-tolerant trees including *Laureliopsis philipiana*, and *Saxegothaea conspicua* (Kitzberger and Veblen 2003). Subalpine forests at elevations above 1000 m elev. are dominated by *N. pumilio*. With the eastward decline in precipitation, *N. dombeyi* forms a homogeneous forest composition with a 3- to 6-m tall, dense Andean bamboo (*Chusquea culeou*) understory. At intermediate precipitation levels and elevation (1500–1000 mm/yr^{-1}; 1000 to 800 m elevation), the conifer *Austrocedrus chilensis* co-dominates with *N. dombeyi* in dry, mixed forest. With increasing aridity (< 1000 mm yr) to the east, open woodland of *A. chilensis* becomes dominant with xeric shrubs such as *Aristotelia chilensis* and *Lomatia hirsuta*. At the forest-steppe ecotone, *A. chilensis* gives way to steppe grasses and small shrubs such as *Discaria articulata* and *Mulinum spinosum*. *N. antarctica* dominates nutrient-limited sites, xeric sites close to the steppe and favors north-facing slopes, riparian areas and bogs with high ground water, disturbed sites, and places exposed to strong winds (Kitzberger and Veblen 2003).

Methods

LPJ-GUESS was run with monthly climate data from the climate research unit (CRU; 1901–2016) to simulate the vegetation of northern Patagonia (Harris et al. 2014). The model was parameterized with the major plant functional types (PFT) and tree species that dominate the study area. We ran six simulations with different parameters that are summarized in Table 2: (1) detrended gridded meteorology for approximately pre-industrial climate conditions (PI; 1901–1930 repeated to run the simulations for 1901–2016) and pre-industrial atmosphereic CO_2 concentration; (2) transient grided meteorology climate (1901–2016) and transient CO_2 concentration; (3) pre-industrial CO_2 value of 280 ppmv; and (4) observed CO_2 values from 1901 to 2016. We implemented a land masking system to eliminate fire in agricultural and urban landscape in a subset of simulations. By using pair-wise combinations, we

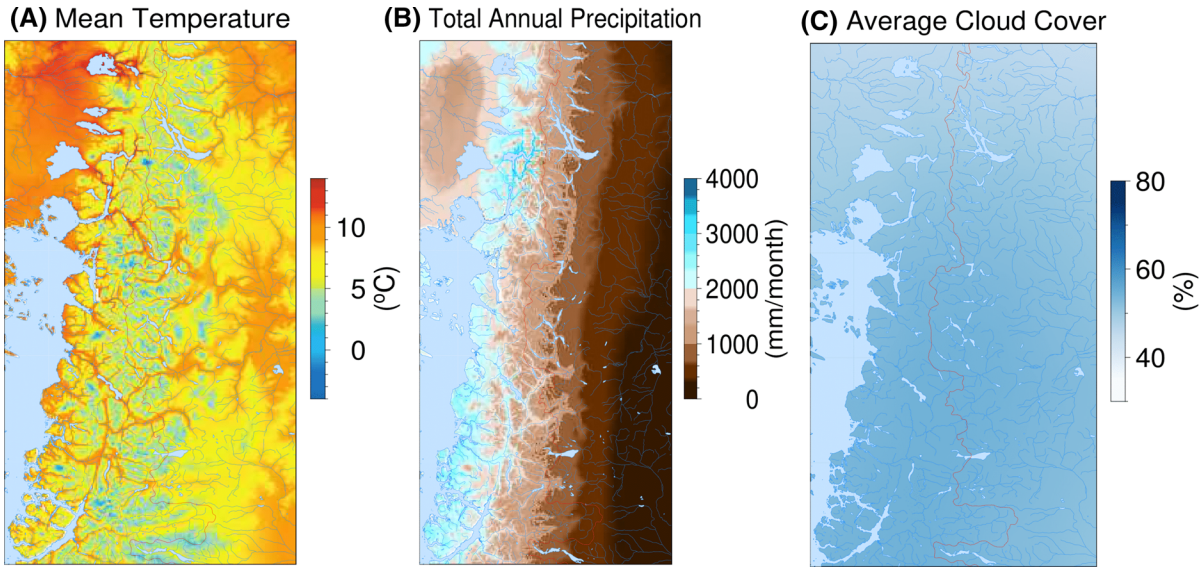

Fig. 2 Spatial distribution of downscaled (1981–2010) CRU climate data (0.008333 resolution). The climate data were downscaled from a 0.5° resolution to a 0.008333° resolution to match the simulated pixels at 0.008333 resolution. **A** mean temperature (°C). **B** annual precipitation (mm/month). **C** mean cloud cover (%). The red line shows the border between Chile and Argentina

were able to quantify the complex and non-linear relationships between climate, CO_2 and fire.

For model evaluation, we compared the simulated above-and below-ground biomass from 2000 to 2013 with remotely sensed derived above-ground biomass (AGB; 2000–2013) (Avitabile et al. 2016), as well as trends in vegetation greenness (Tucker et al. 2010). For fire, we compared model-simulated burned area with MODIS observed burned area (Giglio et al. 2016). Multiple paired *t*-tests on 20000 randomly selected sites were used to determine the extent to which differences between CO_2, fire, and climate drove simulated biomass.

Ecosystem model description

LPJ-GUESS is a DGVM that follows the BIOME3 model (Haxeltine and Prentice 1996). It is designed to model both regional and global vegetation, using a forest gap model in its implementation of plant biophysical properties such as demography and plant resource competition (Bugmann 2001). Model outputs such as biomass, nitrogen balance, and vegetation structure and composition, have been compared with observed data, such as ecosystem flux, field observation, and data inventory associated with net primary pro- ductivity (Kauwe et al. 2014), and remote-sensing data (Blanke et al. 2016). Sensitivity analyses and model-data comparisons suggest that LPJ-GUESS performs well when compared with other terrestrial vegetation models (Sitch et al. 2015).

In LPJ-GUESS, each grid cell is composed of multiple patches (1000 m^2) where individual plant functional types (PFTs) and tree species are simulated. Establishment of each plant functional types (PFTs) and tree species occurs annually, as long as there is low plant density within the grid cell and the simulated climate is within the prescribed bioclimatic limits of the PFT or tree species. The model simulates soil-water content using a two-layer soil hydrology scheme with each layer of a fixed thickness (0.5 m upper and 1.0 m lower thickness) and with percolation between layers, including surface and sub-surface runoff (Haxeltine and Prentice 1996). The model also integrates a process-based fire model called GlobFIRM (Global FIRe Model) to simulate burned area, linking fire with fuel load and fuel moisture, factors that in turn depend on climate and simulated vegetation. Ignitions are assumed to be unlimited, and the area burned is related to fire- season length. The fire effects depend on the length of fire season and the specific fire resistance value for each PFT. In our

simulation, we assumed that the smallest area burned in a grid cell is 1000 m^2 (Thonicke et al. 2001).

Plant functional types and species parameterization

We estimated the bioclimatic parameters associated with the establishment of the six tree species (*Nothofagus dombeyi*, *N. pumilio*, *N. betuloides*, *N. antarctica*, *Fitzroya cupressoides*, *Austrocedrus chilensis*) and two plant functional types (PFTs; Broadleaved evergreen warm temperate trees, Mixed evergreen shrubs) groupings specific to the region, and two grasses (high and low elevation grasses; Table 1), and *Chusquea culeou.* The high-elevation and low-elevation grasses can also be thought of as cool-and warm-temperature grasses, respectively. The bioclimatic parameters are (1) minimum coldest month temperature for survival (T_{cmin_surv}), (2) minimum coldest month mean temperature for establishment (T_{cmin_est}), (3) maximum coldest month mean establishment (T_{wmin_est}) and (4) minimum growing degree days sum on a 5 °C base (GDD_5). GDDs were estimated as a function of monthly mean temperature (Wang et al. 2006) using the equation below:

$$GDD_5 = \sum_{1}^{12} (Tm - 5) \times Nd \; Tm \geq 5^{\circ}\mathrm{C}$$

where GDD_5 is the annual sum of monthly temperature above 5 °C, T_m is the monthly mean temperature (T_m 5 °C), and *N*d is the number of days in a month. In the model, PFT or tree species will not establish in a particular grid cell if the average value of the last 20 years for these variables does not exceed the threshold given in Table 1 (Venevsky et al. 2002). We estimated bioclimatic parameters for each tree species and PFT based on distribution map associated with the classification of southern South America vegetation belts published by the World Wildlife Fund (WWF) (Olson et al. 2001) and Worldclim with a resolution of (~1 km) (Hijmans et al. 2005). The vegetation maps (WWF & Worldclim) classify PFT and tree species into bioclimatic zones that are strongly associated with the distribution of each PFT and tree species. This climate database (WWF & Worldclim) together with monthly means meteorological data from the CRU datasets, were used to create a bioclimatic classification for northern Patagonia and then construct the northern Patagonian bioclimatic natural vegetation distribution maps. The bioclimatic zone for each PFT and tree species was subsequently extracted from the

Table 1 Species parameters and bioclimatic limits used in the simulation: GDD_5; minimum growing degree-day sum (5 °C base), T_{cmin_est} (minimum coldest month mean temperature), T_{cmax_est} (maximum coldest month mean temperature), T_{wmin_est} (minimum warmest month mean temperature), T_{cmin_surv}; (minimum coldest month temperature), D_T; Drought tolerance

Species	GDD_5	T_{cmin_est}	T_{cmax_est}	T_{wmin_est}	T_{cmin_surv}	D_T
High-elevation cool grasses [800–1300 m] (e.g., Cushion grasses)	100	–	0	–	–	–
Low-elevation warm grasses [< 800 m] (e.g., *Stipa speciosa*)	1500	0.6	–	11.6	− 1.3	–
Mixed evergreen shrubs (e.g., *Lomatia hirsuta*, *Schinus patagonicus*)	700	– 0.33	5	10.8	− 3.2	0.59
Broadleaved evergreen warm temperate tree	1500	1.73	7.9	10.1	0.23	0.70
Valdivian forest taxa e.g., *Eucryphia cordifolia*, *Weinmannia trichosperma*						
Austrocedrus chilensis	1350	0.6	6.3	11.6	− 1.3	0.58
Fitzroya cupressoides	600	6.4	0.18	9.3	− 1.4	0.65
Chusquea culeou	700	− 1.6	4.3	8.6	− 3.7	0.62
Nothofagus dombeyi	1000	0.53	8.15	10.9	− 1.4	0.63
Nothofagus pumilio	400	− 1.6	4.3	8.6	− 3.7	0.62
Nothofagus betuloides	1100	0.53	8.15	10.9	− 1.4	0.68
Nothofagus antarctica	700	– 0.36	4.8	10.3	− 2.9	0.58

We use '–' to indicate that no limit is applied

Table 2 The combined effect of climate and CO_2 for each simulation evaluated by the LPJ- GUESS model for the northern Patagonia forest

Model	Climate	CO_2	Fire	Land masking	Scenarios
H–H	Historical	Historical	On	Off	S1
H–H	Historical	Historical	On	On	S2
H–H	Historical	Historical	Off	On	S3
H–PI	Historical	Pre-industrial	On	Off	S4
PI–PI	Pre-industrial	Pre-industrial	On	Off	S5
PI–H	Pre-industrial	Historical	On	Off	S6

H historical climate (1901–2016), *P* pre -industrial climate (1901–1930 recycled for 115 years); historical CO_2: changing CO_2 levels from 1901 to 2016); Pre-industrial CO_2 (constant CO_2 value repeated for 115 years)

vegetation map and overlain on the CRU climate data. We then choose boundary values between 5 and 95% CI for these variables (Table 1) that correspond with the observed limit of each PFT and tree species.

We also focused on fitting parameters related to limiting factors for growth for each tree species and PFT based on the literature and expert advice recieved at workshop with ecologist from Ecotono in San Carlos de Bariloche in 2016. For example, the variables related to drought tolerance (characterized by the minimum ratio of actual transpiration to equilib- rium evapotranspiration) (Sykes et al. 1996) and GDDs were considered the most limiting factors for *Austrocedrus chilensis*. The bioclimatic parameters are listed in Table 1. The parameters used for tree species were based on information about the composition and distribution of native forest in southwestern Argentina and southern Chile (Pollmann and Veblen 2004).

Environmental data and simulation protocol

Present-day vegetation cover was modeled using six experimental scenarios (Table 2) to determine the role of climate, CO_2, and fire. The study was set up using current-era climate data for the "historical period" (1901–2016). LPJ- GUESS began the simulation from "bare ground", (i.e., LPJ-GUESS assumes no vegetation in the grid cells), and the model was run on 100 replicate patches within each grid cell at 1-km^2 (0.008333°) resolution. Each patch has a stochastic element for establishment, mortality, and patch-replacing disturbance, thus allowing the model to represent a quasi-stable landscape pattern and process. The first phase in the simulation is a 1000- years spin-up to achieve equilibrium of pre-industrial stable vegetation structure and carbon pools. For this phase, the first 30 years of detrended historical climate data (1901–1930) were used repeatedly as model input with pre-industrial atmospheric CO_2 content. The detrending of the climate data (1901–1930) was done to remove long-term trends and emphasize short-term (annual to decadal) changes (i.e., variations related to El Niño Southern Oscillation (ENSO) and Southern Annular Mode).

The historical period was simulated following the spin-up and was run from 1901 to 2016 with observed changes in atmospheric CO_2 and climate. The original meteorological data consisted of monthly time series corresponding to mean air temperature, total precipitation and cloud cover percentage at a spatial resolution of 0.5° for the model domain from the climate database CRU TS 4.01 (Harris et al. 2014). The CRU climate data were spatially downscaled and biased-corrected (see Zhang et al. 2017 for details of the downscaling methods) to match the spatial resolution (0.00833°) and historical period of overlap (1960-1990) from the WorldClim-Global Climate Database v1.4 (Hijmans et al. 2005). We compared the performance of the downscaled CRU precipitation and temperature data with the northern patagonia climate grid data (NPCG) (Bianchi et al. 2016). Our results showed good agreement with the NPCG climate data (Supplementary Figure S1). The soil texture data used in the simulations were based on the WISE30sec database (0.00833° spatial resolution) (Batjes 2015), and were used to provide sand, silt and

clay content for estimating water-holding capacity and thermal diffusivity at 1-km^2 resolution.

Experimental design

The simulations summarized in Table 2 examined the effects of individual drivers on vegetation patterns and trends over time (observed CO_2, observed climate, pre-industrial (PI) CO_2 and PI climate; Table 2). A land-masking system was implemented into LPJ-GUESS to ensure that fire did not occur in urban or agricultural areas using data from the land cover data from the Global Land Cover 2000 (GLC2000) for South America (European Commission, Joint Research Center, 2003), which consists of 55 land cover classes at 1- km^2 spatial resolution (Bartholomé and Belward 2007). We classified urban and agricultural grid cells as masked and scaled each 1- km^2 pixel to range between 0 and 1 accordingly. The simulated fire was limited to those areas that were not masked. To assess how well the model represents the biomass gradient in Patagonia (Objective 1), we evaluated it against a biomass map derived from various satellite observations of surface reflectance and vegetation height. For more information see Avitabile et al. (2016). A Pearson correlation coefficient was computed to assess the relationship between the simulated and remotely-sensed biomass. For Objective 2, we used Global Inventory Modeling and Mapping Studies third-generation NDVI (GIMMS NDVI3g) at 8-km^2 resolution for the period of January 1981 to December 2016 based on the Advanced Very High-Resolution Radiometer (AVHRR) sensor to understand regions of browning and greening in the vegetation. The NDVI data are a composite of daily values each half-month (Tucker et al. 2010). NDVI is widely used as a proxy for vegetation productivity and vegetative response to seasonal climate variability (Zhu et al. 2016). Trend analysis on GIMMS NDVI3g was performed using Trend Estimation on annual aggregated time series (AAT) based on Forkel et al. (2013).

We used the modeled carbon in vegetation biomass (Objective 3) from the **S1** scenario (historical climate, changing CO_2, land masking off, fire 'on') and **S4** scenario (historical climate, PI CO_2 (280 ppm), land masking off, fire 'on') to evaluate the effect of CO_2 on forest cover. The difference between the simulations isolates the impact of increasing CO_2 on forest cover compared to the PI level. The same logic was applied to isolate the effect of fire and climate on forest cover. The fire effect was calculated by the difference between **S2** (historical climate, changing CO_2, land masking on, fire 'on') and **S3** (historical climate, historical CO_2, land masking on, fire 'off'). While **S1** and **S6** (PI climate, historical CO_2, land masking off, fire 'on') and **S4** (historical climate, PI CO_2, land masking off, fire 'on') and **S5** (PI climate, PI CO_2, land masking off, fire 'on') were used to calculate the effects of climate. Analysis of the interactions and statistical significance of their effects was determined using paired *t*-tests of difference between the means as estimated for the entire study region. The six experimental set-ups (Table 2) allow for the full evaluation of the individual and combined effect of climate, CO_2, and fire incidence on above-and below-ground biomass.

Lastly, we compared results from Glob-FIRM to the MODIS-observed annual burned area for the period of 2001–2014. The Terra and Aqua combined MCD64A1 Collection 6 sensor Burned Area data product is a monthly, Level-3 gridded 500-m product containing per-pixel burning and quality information. For more information on the MODIS burned area product see Giglio et al. (2018). Finally, the GIMMS NDVI3g and MODIS data were downscaled to 0.00833 (1-km) to match the simulated grid cells.

Results

Overall, the model results show an increase in biomass between 1930 and 2010 based on the S2 (historical climate, historical CO_2, land masking on, fire 'on')

Table 3 This table shows the quantile summary (kg C m^{-2}) for all the scenarios used in these analyses

Model	0%	25%	50%	70%	100%
H–H (S1)	0.00	0.19	2.22	15.7	28.39
Fire (S2)	0.00	0.19	0.65	9.88	29.13
No-FIRE (S3)	0.00	0.19	0.65	10.27	29.06
H–PI (S4)	0.00	0.13	1.67	13.57	24.59
PI–PI (S5)	0.00	0.08	0.42	12.16	23.14
PI–H (S6)	0.00	0.13	0.53	14.17	26.65

simulation (Fig. 4b and Table 3). This increase in biomass is coincident with increased CO_2, warming, and a modest decrease in precipitation (Supplementary Figure 5S) (Harris et al. 2014). In contrast, the simulation with PI CO_2 resulted in decreased forested area under historical climate. PI climate with PI CO_2 reduced forest distribution, but the effect of PI CO_2 alone on biomass was minor compared to the effect of PI climate. However, the absence of fire increased forest biomass under warmer climate, increasing CO_2, and land masking.

The spatial distribution of forests simulated by S2 (historical climate, historical CO_2, masking on, fire 'on') and remotely sensed above-ground biomass (AGB) are shown in Figure 3. The model captured the general observed distribution of present-day vegetation from the temperate rainforest west of the Andes to the mesic forests on the east. The model results underestimate the sharp lower treeline boundary on the eastern side of the Andes and instead showed low simulated biomass in the steppe (Fig. 3a). Simulated biomass ranged from 0 to 29 kg C m^{-2}, whereas remotely sensed observed above-ground biomass ranged between 0 and 48 kg C m^{-2}. There was a positive correlation between the two variables (R^2 = 0.71; simulated mean = 5.68 kg C m^{-2}, observed mean = 7.72 kg C m^{-2}). Overall, there was a strong positive correlation between simulated and observed biomass especially in the temperate forest west of the Andes and the mesic forest at high elevations on both sides of the Andes (Fig. 3a, b).

In S2 (historical climate, historical CO_2, masking on, fire 'on'), high biomass at the mesic forest (high elevation) and forest-steppe ecotone was accompanied by a decrease in the burned-area fraction from 1901 to 2016. However, burned area fraction increased with latitude along the steppe from north to south of the study region (Fig. 4b). In the steppe, mixed patches of high and low burned area are consistent with previous studies that show fuel discontinuity at the steppe (see Fig. 4b).

Analysis of the annual aggregated time series (AAT) GIMMS NDVI dataset from 1982 to 2016 shows a greening trend (mean = +0.17 NDVI units yr^{-1}, $P < 0.05$, standard deviation (SD) = 0.38) for 9.12% of the spatial pixels. However, an observed browning trend (mean = − 0.51 NDVI units yr^{-1}, $P < 0.05$, SD = 0.500) was detected for 46% of the spatial pixels. The mean trend for the entire region was − 0.001027 NDVI yr^{-1}. The high browning percentage was concentrated in steppe vegetation while the greening trend occurred in the mesic forest (Fig. 3c).

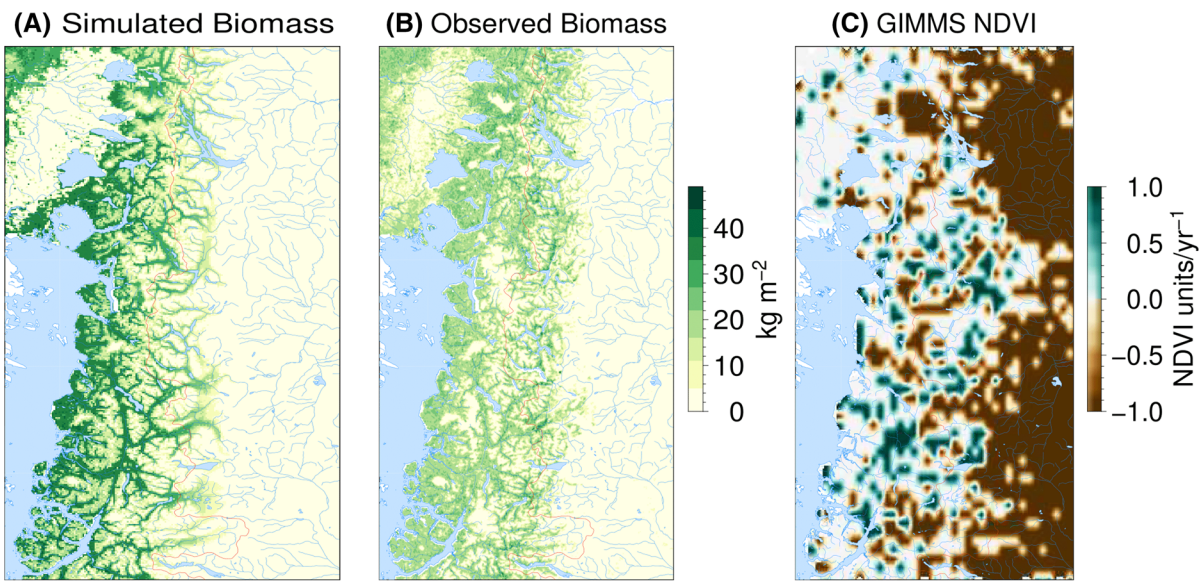

Fig. 3 Spatial distribution of **A** simulated above and below-using S2 (historical climate, historical CO, masking on, fire 'on'); and **B** Avitabile et al. (2016) observed biomass (Kg C m^{-2}); and **C** trends in annual mean NDVI in northern Patagonia from 1982 to 2016. Trend significance was estimated using Forkel et al. (2013). The simulated above-ground biomass is based on S2 (historical climate, historical CO_2, masking on)

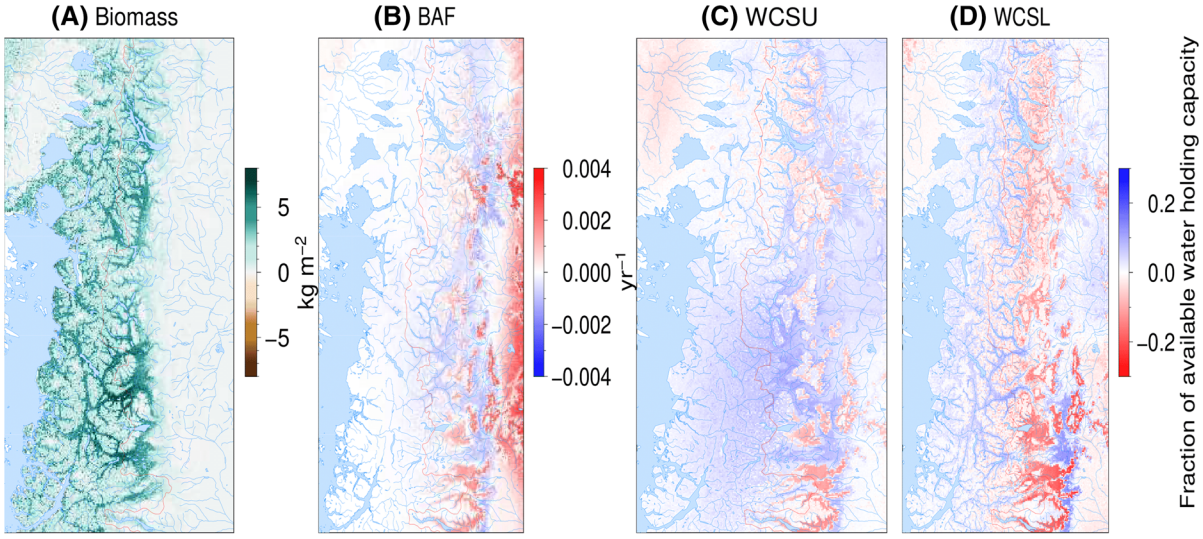

Fig. 4 Changes in metric between 1930 and 2010 from S2 scenario (historical climate, historical CO_2, fire 'on'). Positive values suggest increases and negatives values suggest decreases in **A** average tree biomass (Kg C m^{-2}); **B** average burned-area fraction; **C** upper soil moisture (fraction of available water holding capacity), see legend (**D**), and **D** lower soil moisture (same unit as (**C**)).

Spatial differences in biomass patterns between S1, S4, S5, and S6 simulations

Biomass increased by 22.6% in S1 scenario (historical climate, increasing CO_2, masking off, with fire 'on'), increasing mostly along the forest-steppe ecotone, but also in temperate forest west of the Andes and high-elevation mesic forest. On average, PI CO_2 under warming historical climate (S4) increased simulated tree biomass by 10.4%. In the S4, biomass increased in high-elevation mesic forest and at the forest-steppe ecotone, but a substantial decline in biomass occurred in the temperate forest west of the Andes. The use of S5 (PI climate and low CO_2) produced a realistic reduction in simulated biomass by 1.6% from the temperate forest west of the Andes, to the Patagonia steppe, and also from north to south in the study area (Fig. 5e). However, the use of PI climate with changing CO_2 (S6) increased the simulated biomass by 9.6%. In S6, the most substantial gain in biomass occurred mainly at the temperate forest west of the Andes (Fig. 5f and Table 3).

Influence of fire on vegetation

Figure 6 shows the results of simulated LPJ-GUESS burned area for S2 and the observed burned area from MODIS. Although the model overestimatesburned area, the simulations showed similar trends to the MODIS data. Fire plays a significant role in the reduction of biomass. The small area burned or absence of fire in all the simulations in temperate forest west of the Andes and the mesic forest at high elevations is mainly related to water availability because high effective moisture increases soil water content and makes the forest naturally fire resistant. Moving into the transition zone between the forest and grassland, the magnitude of fire increased because of a decrease in soil moisture (Fig. 7).

To assess the effect of CO_2 on simulated biomass, two sets of combinations (S1–S4 and S6–S5) were analyzed. The difference between S1 (historical climate, increasing CO_2, land mask off, with fire 'on') and S4 (historical climate and PI CO_2, land mask off, with fire 'on') overall shows increased forest productivity (Fig. 8a). The results of the paired *t*-test between S1 and S4 indicated that the inclusion of changing CO_2 in S1 was responsible for the increase in average biomass (M = 1.03 kg m^{-2}; t (19999) = 100.31, $P < 0.01$) due to CO_2 fertilization. Consequently, the effect of low CO_2 thus reduces more biomass at the forest-steppe compared to the temperate forest west of the Andes, and the mesic forest (high elevation). Also, the difference between S6 (PI climate, changing CO_2) and S5 (PI climate, PI CO_2) shows increases (M = 0.93 kg m^{-2}; t (19999) = 94.65,

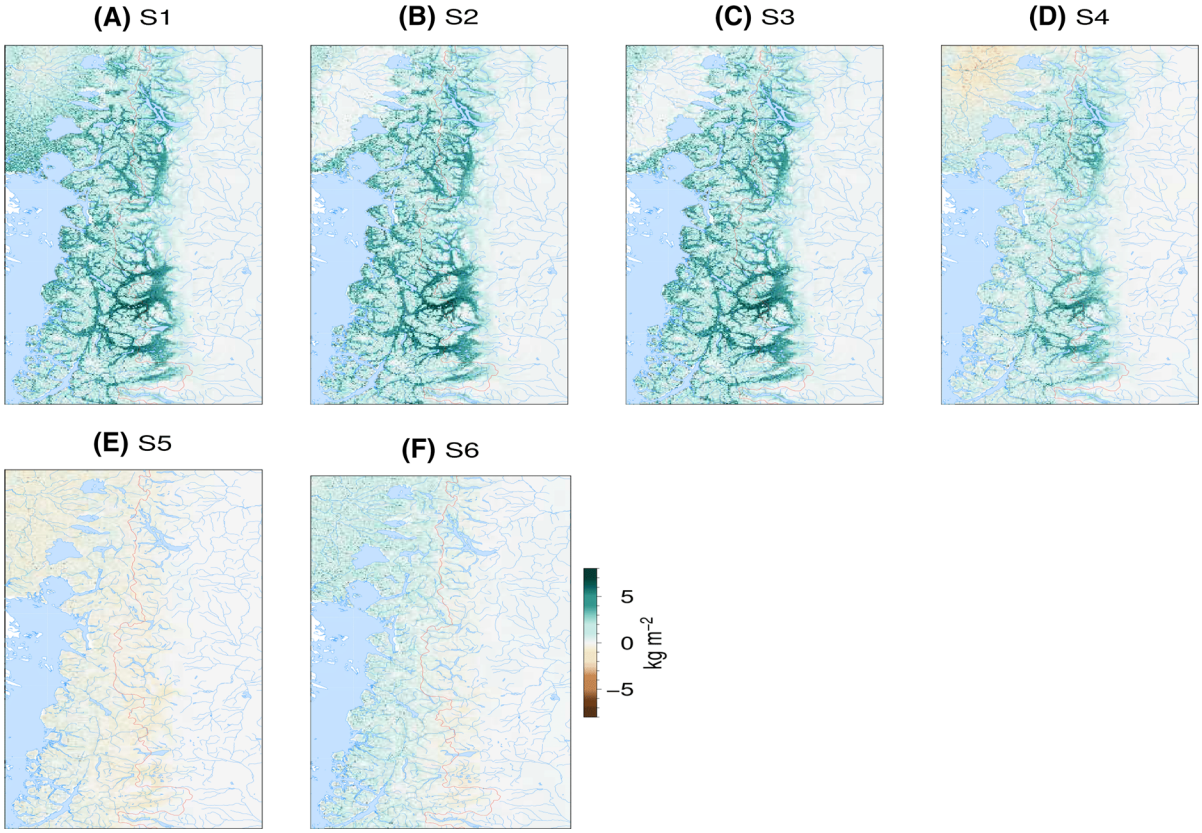

Fig. 5 The mean biomass change between 1930 and 2010 (difference between the time periods). Positive values suggest high biomass and negative values suggests low biomass. **A** S1 (historical climate, historical CO_2); **B** S2 (historical climate, historical CO_2, masking on); **C** S3 (historical climate, historical CO_2, masking on, fire off); **D** S4 (historical climate, PI CO_2); **E** S5 (PI climate, PI CO_2); and) S6 (PI climate, historical CO_2)

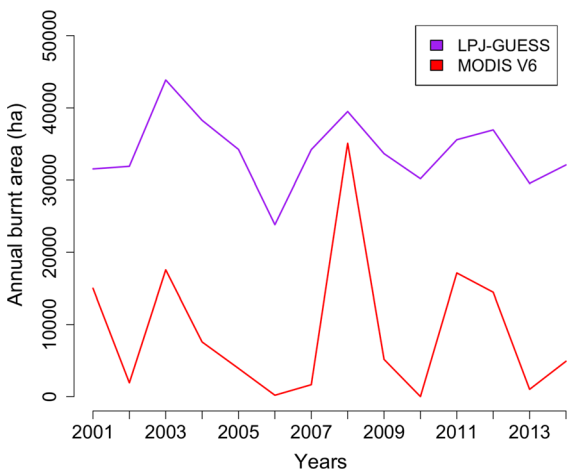

Fig. 6 Mean annual burned area from 2001 to 2014 in northern Patagonia showing output from MOIDS V6 and LPJ-GUESS model. The output from LPJ-GUESS was from the S2 simulation (historical climate, historical CO_2, masked on, fire 'on')

$P < 0.01$) in biomass caused by CO_2 fertilization which increase the biomass stock (Fig. 8b). These results show that the inclusion of changing CO_2 partially explains recent increases in forest productivity.

The effect of climate was analyzed based on two combinations (S4–S5 and S1–S6). The comparison between the mean of S4 (historical climate and PI CO_2) and S5 (PI climate and PI CO_2) shows an increase in biomass under changing climate (M = 0.82 kg m^{-2}; t (19999) = 76.47, $P < 0.01$). Simulated biomass increased the most in mesic forest and along the forest-steppe ecotone with warming climate. The effect of climate based on the difference between S1 (historical climate and historical CO_2) and S6 (PI climate and changing CO_2) reveal the same spatial pattern as S4–S5 (Fig. 2d, e). The presence of warming climate increased simulated average biomass (M= 0.918 kg m^{-2}; t (19999) = 76.74, $P < 0.01$)

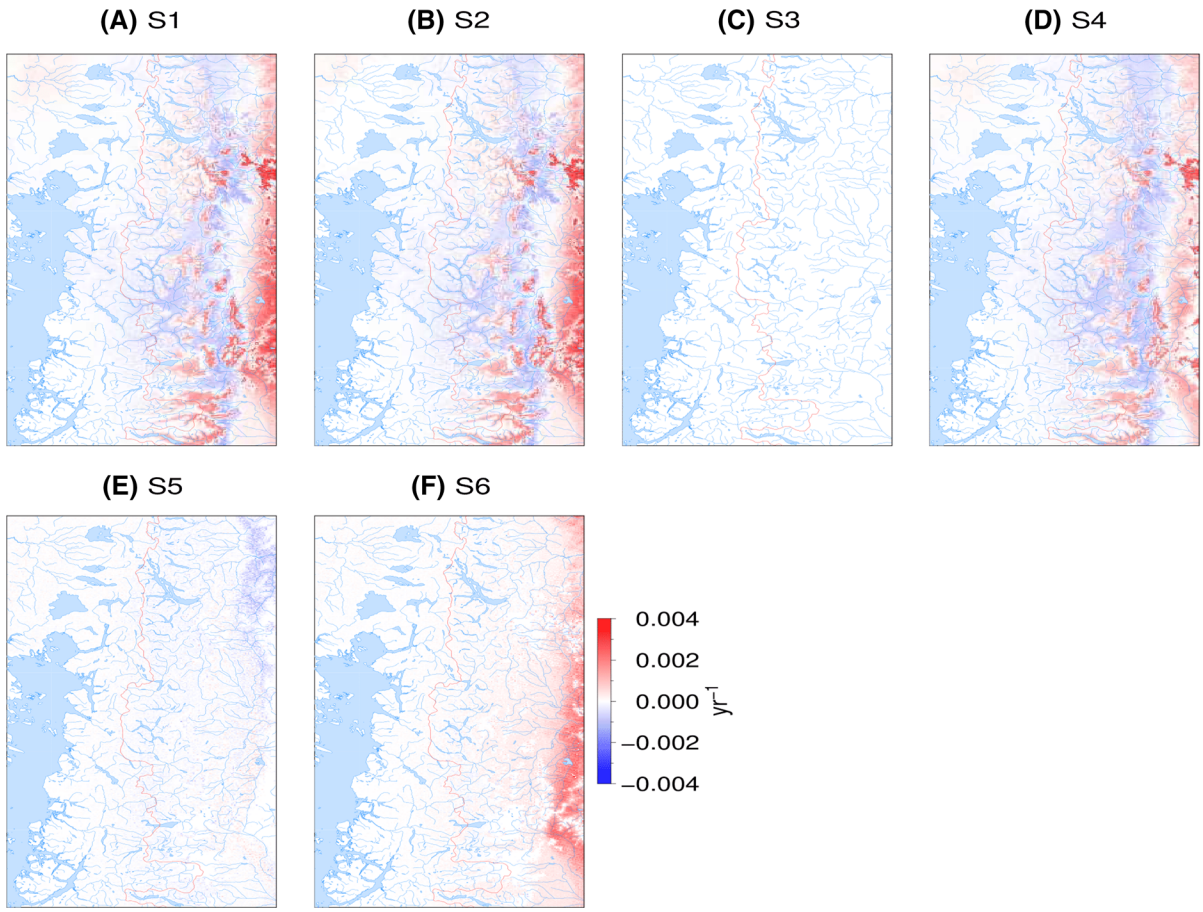

Fig. 7 Maps of mean burned area fraction between 1930 and 2010 (difference between the periods). Positive values suggest region of high fire activity and negative values suggests regions of low fire activity. **A** S1 (historical climate, historical CO_2); **B** S2 (historical climate, historical CO_2, masking on); **C** S3 (historical climate, historical CO_2, masking on, fire 'off'); **D** S4 (historical climate, PI CO_2); **E** S5 (PI climate, PI CO_2); and **F** S6 (PI climate, historical CO_2)

The spatial difference between S2 (historical climate, increasing CO_2 masking on, with fire 'on') and S3 (historical climate, increasing CO_2, land masking on, with fire 'off') reveal biomass loss throughout the study region (Fig. 8c). The inclusion of fire reduced forest cover compared to the absence of fire ($M = -0.21$ kg m^{-2}; $t\ (19999) = -29.93$, $P < 0.01$).

Discussion

Our study provides the first attempt to use a DGVM to simulate drivers of forest cover change in southern South America. The incorporation of 20th century atmospheric CO_2 concentrations, climate, and fire in LPJ- GUESS allows for the assessment of their relative influence on the simulated vegetation structure and dynamics of the northern Patagonia (Fig. 5a). However, the interactions at high and low elevations, including at the forest- steppe ecotone, have seldom been considered before. The results suggest that climate, CO_2, and fire play a crucial role in determining the long-term vegetation dynamics. Our results show (Fig. 5a) that (1) increased temperature and atmospheric CO_2 concentration likely increased forest growth, as CO_2 induced reduction in stomatal conductance, increased water use efficiency (WUE); and (2) fire is an important disturbance process along the ecotone where Andean forest meets Patagonia steppe (Fig 7). Our results are broadly consistent with other forest models that demonstrate a positive relationship

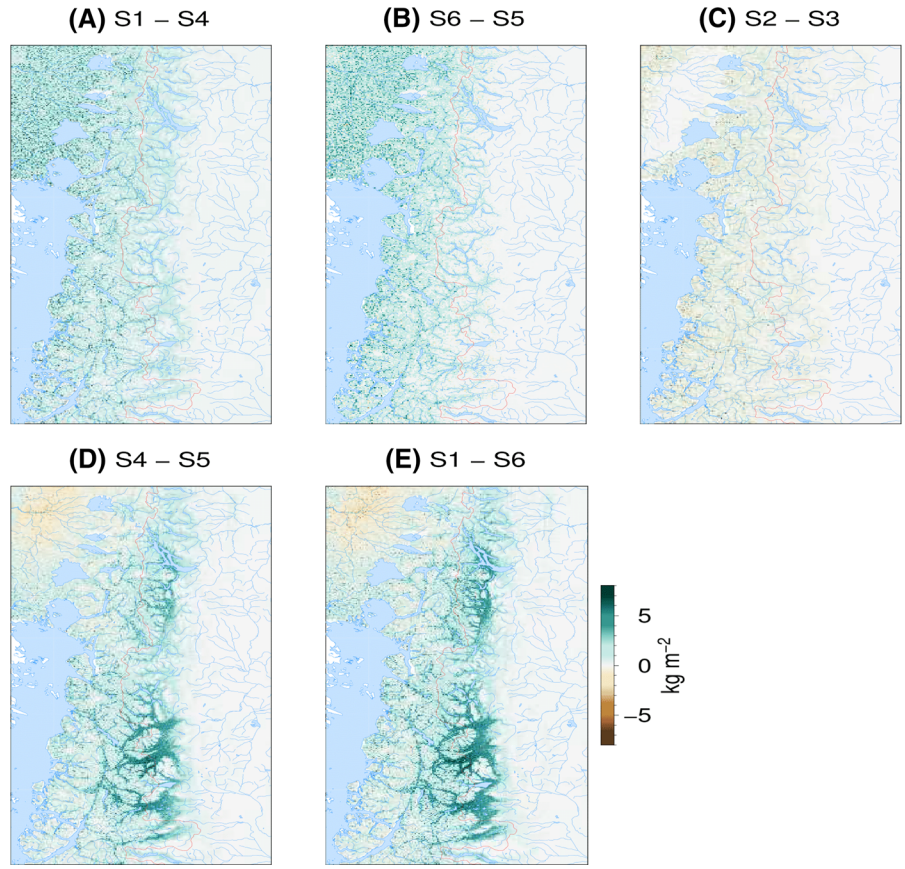

Fig. 8 Effect of CO_2, fire, and climate on forest cover. The figure show changes in metric between 1930 and 2010 (difference between the time periods). **A**, **B** shows the effect of CO_2: (**A**) (S1: historical climate, historical CO_2) minus S4 (historical climate, low CO_2); **B** (S6: PI climate, changing CO_2 minus S5: PI climate, PI CO_2). **C** shows the effect of fire (S2: historical climate, historical CO_2, masking on, with fire 'on') minus S3 (historical climate, historical CO_2, masking on, with fire 'off'). **D**, **E** shows the effect of climate (**D**) (S4: historical climate, low CO_2) minus (S5: PI climate, low CO_2); **E** (S1: historical climate, historical CO_2) minus (S6: PI climate, historical CO_2). Positive values suggest regions of increasing biomass and negative values suggests region of decreasing biomass

between increased CO_2 and forest productivity (Hickler et al. 2015), and with observations that fire activity in the region has changed with warming and drying climate (Kitzberger and Veblen 2003).

Changes in forest cover

The results from S4 (historical climate and low CO_2), S5 (PI climate and low CO_2), and S6 (PI climate and historical CO_2; Fig. 5d–f) show lower biomass than S2, which supports studies that suggest that CO_2 limits forest expansion into grasslands (Hirota et al. 2011). The significant greening and browning trends (1982–2016) occurred in 9.12 and 46% of the natural vegetation of northern Patagonia, with 44% of the remaining pixels showing no significant change. The strong greening trend occurred in the mesic forest (high elevation) and forest-steppe (low elevation) biomes, while the strong browning trend was more pronounced at the semi-arid steppe (Fig. 3c).

The differences between 1930 and 2010, as simulated in S2 (historical climate and historical CO_2), revealed that biomass increased throughout northern Patagonia. The increase in biomass at the forest-steppe ecotone coincided with a decrease in the fraction of burned area and decrease in soil moisture at the forest-steppe (Fig. 4b–d). Our results suggest that increased CO_2 fertilization, and warmer climate, and decreased fire frequency caused forests to expand throughout northern Patagonia. This differs from previous research that attributes forest expansion to intentional fire suppression at the forest-steppe ecotone (Veblen and Lorenz 1987; Veblen and Lorenz 1988; Kitzberger and Veblen 2003; Gowda et al. 2011). Despite the observed decline in precipitation and increase in temperature in northwestern Patagonia since the 1940s based on CRU data analysis supplementary Figure 5S (Veblen et al. 2011).

In general, our model accurately simulated the closed canopy forests west of the Andes and the mesic forest at high elevation, but it did not produce the sharp

change between forest and steppe biomes along the forest-steppe ecotone. The poor result along the ecotone might be attributed to the two-layer soil hydrology architecture of the model, which lacked ground water storage for a semi-arid ecosystem (Wramneby et al. 2008). A lack of ground water storage might reduce the capacity of steppe vegetation to extract the water required for photosynthesis during the dry season from October to March (Hickler et al. 2004). The simulated low fire activity in S5 and S6 suggested that the lack of interannual climate variability was significant to decrease fire.

Influence of CO_2, fire, and climate on Patagonia forest

Spatial analysis and paired *t-tests* show that climate and CO_2 had greater influences on biomass than fire (Fig. 8b, c). The effect of CO_2, fire and, climate simulated by our model supports previous studies that compared the influence of low CO_2 and warmer climates on global biome distribution (Calvo and Prentice 2015). The effect of PI CO_2 (S1–S4) on modern climate was more visible at the forest-steppe ecotone, where biomass was low. The comparison between S1 (changing climate, changing CO_2) & S4 (changing climate, PI CO_2), and S6 (PI climate, changing CO_2) & S5 (PI climate, PI CO_2) shows the physiological effect of CO_2 fertilization on forest productivity. With the physiological effects of CO_2 turned on, the model projected an increase in biomass for both paired comparisons. The physiological effect of CO_2 on vegetation productivity has mainly been observed in modeling studies due to limited observational data (Hickler et al. 2015). The comparison of S1 (changing climate and CO_2) with S4 (changing climate and PI CO_2), and S6 (PI climate and changing CO_2) with S5 (PI climate and CO_2) shows the physiological effects of CO_2 fertilization on forest productivity. With the physiological effects of CO_2 turned on, the model projected an increase in biomass for both paired comparisons. Our S5 simulation shows that fire amplifies the interaction between climate and CO_2 leading to a large reduction in biomass under a combination of PI climate and PI CO_2 (Fig. 8b). This combination reduced the ability of forest to expand due to fire disturbance.

Fire controls biomass dynamics in an ignition-limited ecosystem such as the Patagonia mesic forest (Kitzberger et al. 2016). The large difference in the amount of hectares burned between the simulated and the observed is due to the assumption of unlimited ignition in Glob-FIRM, where as long as the fuel load is above 200 g/m^2 fire will occur. The assumption however is not true in an ignition-limited ecosystems such as northern Patagonia, where natural ignitions are infrequent. The simulated cessation of fire caused biomass to increase under S3 (historical climate, changing CO_2, masking on, with fire 'off'). The comparison between S2 and S3 shows that the presence of fire decreased biomass and that in the absence of fire there was a longer rate of biomass turnover (Fig. 5b, c). Nonetheless, our simulation using historical climate and changes in CO_2 show that fire amplified the biomass response to CO_2 under changes in climate variability (e.g., ENSO) due to rapid fuel increase in fuel. This result is consistent with Bond and Keeley (2005). Fire studies at the forest-steppe ecotone thus show the importance of changes in fire frequency and severity on the rate of biomass turnover (Veblen et al. 1999). Fewer fires in scenario S1, S2, and S3 resulted in high biomass and forest expansion (Fig. 2a–c). Simulations including interannual climate variability show an impressive reduction in temperate rainforest biomass during periods of prolonged drought (Fig. 8d, e). The results from this study, which documents the sensitivity of temperate rainforest to warming trends provide additional insight into the drivers of terrestrial ecosystem dynamics.

Conclusion

Research presented here suggests that LPJ-GUESS can realistically simulate recent responses of northern Patagonia forests to changes in CO_2, climate, and fires. The similarity between the simulated biomass and observed biomass of temperate rainforest west of the Andes and mesic forests east of the Andes shows that the model can capture local vegetation and dynamics. Significant findings from this study are:

1. Under current climate condition and rising CO_2, the model predicts increased in forest cover with a concomitant increase in fire activities.
2. By contrast the simulation that used pre-inustrial CO_2 and pre- industrial climate resulted in

decreased forested area throughout northern Patagonia.
3. A simulated increase in fire activity was a result of increasing fuel load, warmer temperature, and drier conditions.
4. Simulations show that climate was the strongest simulated driver of forest expansion and CO_2 fertilization was the second most important driver.

In order to improve the accuracy of LPJ-GUESS at the patch level, it is necessary to improve the parameterization of the key taxa. This effort will include more sensitivity analyses on some critical parameters, such as distance to seed source as well as the establishment conditions that differ widely in closed forests as compared to forest expansion. These factors may not be important in long-term studies but have a strong effect in the time frame of this study (100 years), particularly for species such as *N. pumilio*, that exhibited clear difficulty reestablishing following disturbance. Moreover, there are limited model simulations that examine long-term forest cover trends and how environmental factors, such as climate and CO_2 affect regional vegetation change through fire (Dionizio et al. 2018). Thus, this new parameterization of the important regional tree species will be useful for understanding past and future vegetation changes in the study area.

Acknowledgements Research was supported by National Science Foundation grants GSS 1461590. We thank T. Kitzberger, J. Paritsis, J. Gowda for their helpful suggestions in improving the manuscript and also for their contribution in parameterizing PFTs, tree species and grasses used for LPJ-GUESS simulation during the 2016 spring workshop in Bariloche, Argentina. This paper also benefited from the comments of Laura Burkle (Department of Ecology, Montana State University, Bozeman, USA)

Author contributions All authors contributed to the final manuscript. AO designed the research, processed the data, discussed the results, and contributed to the writing of the manuscript, JK contributed to the analysis of the results. CW contributed to funding the study, discussing results, and editing of the manuscript, WN contributed to the editing of the manuscript and discussing the results, BP contributed to funding the study, analysis of results and writing of the manuscript, DR contributed to the writing and analysis of the results. All authors discussed the results and drew the conclusions.

Funding This research was supported by the National Science Foundation Grant GSS 1461590.

Declarations

Conflict of interest The authors declared no conflict of interest.

References

AmingoRamirez JC (1998) A bioclimatic classification of Chile: woodland comunities in the temperate zone. Plant Ecol 136:9–26

Avitabile V, Herold M, Heuvelink GBM, Lewis SL, Phillips OL, Asner GP, Armston J, Ashton PS, Banin L, Bayol N, Berry NJ, Boeckx P, Jong BHJ, DeVries B, Girardin CAJ, Kearsley E, Lindsell JA, Lopez-Gonzalez G, Lucas R, Malhi Y, Morel A, Mitchard ETA, Nagy L, Qie L, Quinones MJ, Ryan CM, Ferry SJW, Sunderland T, Laurin GV, Gatti RC, Valentini R, Verbeeck H, Wijaya A, Willcock S (2016) An integrated pan-tropical biomass map using multiple reference datasets. Glob Change Biol 22(4):1406–1420.

Bartholomé E, Belward AS (2007) GLC2000: a new approach to global land cover mapping from Earth observation data. Int J Remote Sens 26:1959–1977

Batjes NH (2015) World soil property estimates for broad-scale modellling (WISE30sec,ver.1.0). Report 2015/01, ISRIC - World Soil Information, Wageningen

Bianchi E, Villalba R, Viale M, Couvreux F, Marticorena R (2016) New precipitation and temperature grids for northern Patagonia: advances in relation to global climate grids. Journal of Meteorological Research 30(1):38–52.

Blanke JH, Lindeskog M, Lindström J, Lehsten V (2016) Effect of climate data on simulated carbon and nitrogen balances for Europe. J Geophys. Cal Res. Biogeosci. 121(5):1352–1371.

Bond W, Keeley J (2005) Fire as a global 'herbivore': the ecology and evolution of flammable ecosystems. Trends Ecol Evol 20(7):387–394.

Bradshaw RHW, Sykes MT (2014) From the past to the future. Wiley-Blackwell, p 334

Bugmann H (2001) A review of forest gap models. Clim Change 51:259–305

Calvo MM, Prentice IC (2015) Effects of fire and CO2 on biogeography and primary production in glacial and modern climates. New Phytol 208:987–994

Dionizio EA, Costa MH, de Almeida Castanho AD, Pires GF, Marimon BS, Marimon-Junior BH, Lenza E, Pimenta FM, Yang X, Jain AK (2018) Influence of climate variability, fire and phosphorus limitation on vegetation structure and dynamics of the Amazon-Cerrado border. Biogeosciences 15(3):919–936.

Forkel M, Carvalhais N, Verbesselt J, Mahecha M, Neigh C, Reichstein M (2013) Trend change detection in NDVI time series: effects of inter- annual variability and methodology. Remote Sensing 5(5):2113–2144.

Garreaud RD, Vuille M, Compagnucci R, Marengo J (2009) Present-day South American climate. Palaeogeogr Palaeoclimatol Palaeoecol 281(3–4):180–195.

Garreaud R, Lopez P, Minvielle M, Rojas M (2013) Large-scale control on the patagonian climate. J Clim 26(1):215–230.
Giglio L, Boschetti L, Roy DP, Humber ML, Justice CO (2018) The collection 6 MODIS burned area mapping algorithm and product. Remote Sens Environ 217:72–85.
Giglio L, Schroeder W, Justice CO (2016) The collection 6 MODIS active fire detection algorithm and fire products. Remote Sensing of Environ 178:31–41.
Harris I, Jones PD, Osborn TJ, Lister DH (2014) Updated high-resolution grids of monthly climatic observations—the CRU TS3.10 dataset. Inter J Climatol 34(3):623–642.
Haxeltine A, Prentice IC (1996) BIOME3: an equilibrium terrestrial bio- sphere model based on ecophysiological constraints, resource availability, and competition among plant functional types. Global Biogeochem Cycles 10(4):693–709.
Hickler T, Smith B, Sykes MT, Davis MB, Sugita S, Walker K (2004) Using a generalized vegetation model to simulate vegetation dynamics in northeastern usa. Ecology 85(2):519–530.
Hickler T, Rammig A, Werner C (2015) Modelling CO2 impacts on forest productivity. Curr for Reports 1(2):69–80.
Hijmans RJ, Cameron SE, Parra JL, Jones PG, Jarvis A (2005) Very high resolution interpolated climate surfaces for global land areas. Inter J Climatol 25(15):1965–1978.
Hirota M, Holmgren M, Nes EHV, Scheffer M (2011) Global resilience of tropical forest and savanna to critical transitions. Science 334(6053):232–235.
Gowda JH, Kitzberger T, Premoli AC (2011) Landscape responses to a century of land use along the northern Patagonian forest-steppe transition. Plant Ecol 213:259–272. https://doi.org/10.1007/s11258-011-9972-5
Kauwe MGD, Medlyn BE, Zaehle S, Walker AP, Dietze MC, Wang YP, Luo Y, Jain AK, El-Masri B, Hickler T, Wårlind D, Weng E, Parton WJ, Thornton PE, Wang S, Prentice IC, Asao S, Smith B, McCarthy HR, Iversen CM, Hanson PJ, Warren JM, Oren R, Norby RJ (2014) Where does the carbon go? A model–data intercomparison of vegetation carbon allocation and turnover processes at two temperate forest free-air CO2 enrichment sites. New Phytol 203(3):883–899.
Kitzberger T, Veblen TT (2003) Influence of climate on fire in northern Patagonia, Argentina. In: Baker WL, Montenegro G, Swetnam TW (eds) Fire regimes and climatic change in temperate ecosystem of the western Americas. Springer-Verlag, Berlin
Kitzberger T, Perry GLW, Paritsis J, Gowda JH, Tepley AJ, Holz A, Veblen TT (2016) Fire–vegetation feedbacks and alternative states: common mechanisms of temperate forest vulnerability to fire in southern South America and New Zealand. N Z J Bot 54(2):247–272
Kottek M, Grieser J, Beck C, Rudolf B, Rubel F (2006) World map of the Köppen-Geiger climate classification updated. Meteorol Z 15(3):259–263.
Olson DM, Dinerstein E, Wikramanayake ED, Burgess ND, Powell GVN, Underwood EC, Damico JA, Itoua I, Strand HE, Morrison JC, Loucks CJ, Allnutt TF, Ricketts TH, Kura Y, Lamoreux JF, Wettengel WW, Hedao P, Kassem KR (2001) Terrestrial ecoregions of the world: a new map of life on earth. Bioscience 51(11):933–933.
Paritsis J, Landesmann J, Kitzberger T, Tiribelli F, Sasal Y, Quintero C, Dimarco R, Barrios-García M, Iglesias A, Diez J, Sarasola M, Nuñez M (2018) Pine plantations and invasion alter fuel structure and potential fire behavior in a patagonian forest-steppe ecotone. Forests 9
Paruelo JM, Beltran AB, Jobbagy EG, Sala OE, Golluscio RA (1998) The climate of Patagonia: general patterns and controls on biotic processes. Ecol Aust 8:85–101
Pollmann W, Veblen TT (2004) Nothofagus regeneration dynamics in south-central Chile: a test of a general model. Ecol Monogr 74(4):615–634.
Sitch S, Friedlingstein P, Gruber N, Jones SD, Murray-Tortarolo G, Ahlström A, Doney SC, Graven H, Heinze C, Huntingford C, Levis S, Levy PE, Lomas M, Poulter B, Viovy N, Zaehle S, Zeng N, Arneth A, Bonan G, Bopp L, Canadell JG, Chevallier F, Ciais P, Ellis R, Gloor M, Peylin P, Piao SL, Quéré CL, Smith B, Zhu Z, Myneni R (2015) Recent trends and drivers of regional sources and sinks of carbon dioxide. Biogeosciences 12(3):653–679.
Sykes MT, Prentice IC, Cramer W (1996) A bioclimatic model for the potential distributions of north European tree species under present and future climates. J Biogeogr 23:203–233
Thonicke K, Venevsky S, Sitch S, Cramer W (2001) The role of fire disturbance for global vegetation dynamics: coupling fire into a dynamic global vegetation model. Glob Ecol Biogeogr 10(6):661–677.
Tucker CJ, Pinzon JE, Brown ME, Slayback DA, Pak EW, Mahoney R, Vermote EF, Saleous NE (2010) An extended AVHRR 8-km NDVI dataset compatible with MODIS and SPOT vegetation NDVI data. Int J Remote Sens 26:4485–4498
Van der Werf GR, Randerson JT, Giglio L, Collatz GJ, Mu M, Kasibhatla PS, Morton DC, DeFries RS, Jin YV, van Leeuwen TT (2010) Global fire emissions and the contribution of deforestation, savanna, forest, agricultural, and peat fires (1997-2009). Atmos Chem Phys 10:1170. https://doi.org/10.5194/acp-10-11707-2010
Veblen TT, Lorenz DC (1988) Recent vegetation changes along the forest/steppe ecotone of northern Patagonia. Ann Assoc Am Geogr 78(1):93–111.
Veblen TT, Donoso C, Kitzberger T, Rebertus AJ (1996) Ecology of southern chilean and argentinean nothofagus forests. In: Hill RS, Read J (eds) The ecology and biogeography of nothofagus forests. Yale University Press, New Haven
Veblen TT, Holz A, Paritsis J, Raffaele E, Kitzberger T, Blackhall M (2011) Adapting to global environmental change in Patagonia: What role for disturbance ecology? Austral Ecol 36(8):891–903.
Veblen TT, Kitzberger T, Villalba R, Donnegan J (1999) Fire history in northern Patagonia: the roles of humans and climatic variation. Ecol Monogr 69(1):47–67
Venevsky S, Thonicke K, Sitch S, Cramer W (2002) Simulating fire regimes in human-dominated ecosystems: Iberian peninsula case study. Glob Change Biol 8(10):984–998.
Wang T, Hamann A, Spittlehouse DL, Aitken SN (2006) Development of scale-free climate data for Western Canada for use in resource management. Int J Climatol 26(3):383–397.

Wramneby A, Smith B, Zaehle S, Sykes MT (2008) Parameter uncertainties in the modelling of vegetation dynamics—effects on tree community structure and ecosystem functioning in European forest biomes. Ecol Model 216(3–4):277–290.

Zhang Z, Zimmermann NE, Stenke A, Li X, Hodson EL, Zhu G, Huang C, Poulter B (2017) Emerging role of wetland methane emissions in driving 21st century climate change. Proc Natl Acad Sci 114(36):9647–9652. https://doi.org/10.1073/pnas.1618765114

Zhu Z, Piao S, Myneni RB, Huang M, Zeng Z, Canadell JG, Ciais P, Sitch S, Friedlingstein P, Arneth A, Cao C, Cheng L, Kato E, Koven C, Li Y, Lian X, Liu Y, Liu R, Mao J, Pan Y, Peng S, Peñuelas J, Poulter B, Pugh TAM, Stocker BD, Viovy N, Wang X, Wang Y, Xiao Z, Yang H, Zaehle S, Zeng N (2016) Greening of the earth and its drivers. Nat Clim Chang 6:791–795